

## Northern hemisphere cold air outbreaks are more likely to be severe during weak polar vortex conditions

Jinlong Huang <sup>1,2</sup>, Peter Hitchcock <sup>2</sup>✉, Amanda C. Maycock <sup>3</sup>, Christine M. McKenna <sup>3</sup> & Wenshou Tian <sup>1</sup>✉

Severe cold air outbreaks have significant impacts on human health, energy use, agriculture, and transportation. Anomalous behavior of the Arctic stratospheric polar vortex provides an important source of subseasonal-to-seasonal predictability of Northern Hemisphere cold air outbreaks. Here, through reanalysis data for the period 1958–2019 and climate model simulations for preindustrial conditions, we show that weak stratospheric polar vortex conditions increase the risk of severe cold air outbreaks in mid-latitude East Asia by 100%, in contrast to only 40% for moderate cold air outbreaks. Such a disproportionate increase is also found in Europe, with an elevated risk persisting more than three weeks. By analysing the stream of polar cold air mass, we show that the polar vortex affects severe cold air outbreaks by modifying the inter-hemispheric transport of cold air mass. Using a novel method to assess Granger causality, we show that the polar vortex provides predictive information regarding severe cold air outbreaks over multiple regions in the Northern Hemisphere, which may help with mitigating their impact.

<sup>1</sup>College of Atmospheric Sciences, Lanzhou University, Lanzhou, China. <sup>2</sup>Department of Earth and Atmospheric Sciences, Cornell University, Ithaca, NY, United States. <sup>3</sup>School of Earth and Environment, University of Leeds, Leeds, UK. ✉email: [aph28@cornell.edu](mailto:aph28@cornell.edu); [wstian@lzu.edu.cn](mailto:wstian@lzu.edu.cn)

Many major winter weather disruptions in the northern extratropics are associated with cold air outbreaks (CAOs). In particular, severe CAOs are linked to widespread extreme cold temperatures in heavily populated areas of the northern extratropics (Fig. 1a–c), and frequently cause significant travel disruption, economic losses, and fatalities<sup>1–3</sup>. For instance, the severe CAO in February 2018 (Fig. 1a), nicknamed “the Beast from the East” by the media, caused up to 8260 collisions on Britain’s roads in just three days, billions of pounds in economic losses in the UK, and 95 deaths across Europe<sup>4–6</sup>. It is therefore important to understand the determinants of CAOs not only for improving weather forecast skills but also for decision-making.

The Arctic stratospheric polar vortex (hereafter referred to as the polar vortex) is known to affect Northern Hemisphere winter weather on subseasonal-to-seasonal timescales<sup>7–11</sup>. Persistent anomalies in the polar vortex strength are associated with a robust and persistent regional surface weather response in the northern extratropics<sup>12–15</sup> and are known to affect the occurrence of CAOs<sup>16–18</sup>. The forecasting community has therefore suggested that the polar vortex provides useful information for improving subseasonal-to-seasonal forecasts of Northern Hemisphere regional weather<sup>19–23</sup>. However, a lack of one-to-one relationship between the polar vortex strength and the occurrence of CAOs<sup>24,25</sup>, and the complexity of the physical mechanisms responsible for the polar vortex impacting CAOs in the northern extratropics, make it challenging to account for this effect in

forecasts. Moreover, little is known about how the polar vortex affects the severity of CAOs, which is crucial as the societal impacts are often non-linear with substantially larger disruption occurring for more severe CAOs<sup>1,3</sup>. Here we quantify the relationship between a weakened polar vortex and the severity of CAOs in the northern extratropics. We demonstrate further that the weakened polar vortex is followed by a weakened transport of cold air mass across the Arctic Ocean from the Eastern Hemisphere to the Western Hemisphere. This leads to an excess of cold air in high latitudes of Europe and East Asia and sheds light on the spatial and temporal response of CAOs following anomalous stratospheric conditions.

## Results

**Relationship between the polar vortex and severe CAOs.** Our analysis reveals that weak polar vortex conditions are associated with a disproportionate increase in the simultaneous occurrence of severe CAOs in multiple regions of the northern extratropics in a reanalysis dataset, as compared to moderate CAOs (Fig. 1). The definition of a “severe” or “moderate” CAO considers both the geographic extent and the magnitude of the surface temperature anomalies (see “Methods” for definitions and Supplementary Tables 1 and 2 for the total number of CAOs). We identify weak polar vortex days based on the 100-hPa zonal wind anomalies (see “Methods”), which is a method also used in other studies examining stratosphere-troposphere coupling<sup>26,27</sup>. Studies have shown that lower stratospheric anomalies are more important

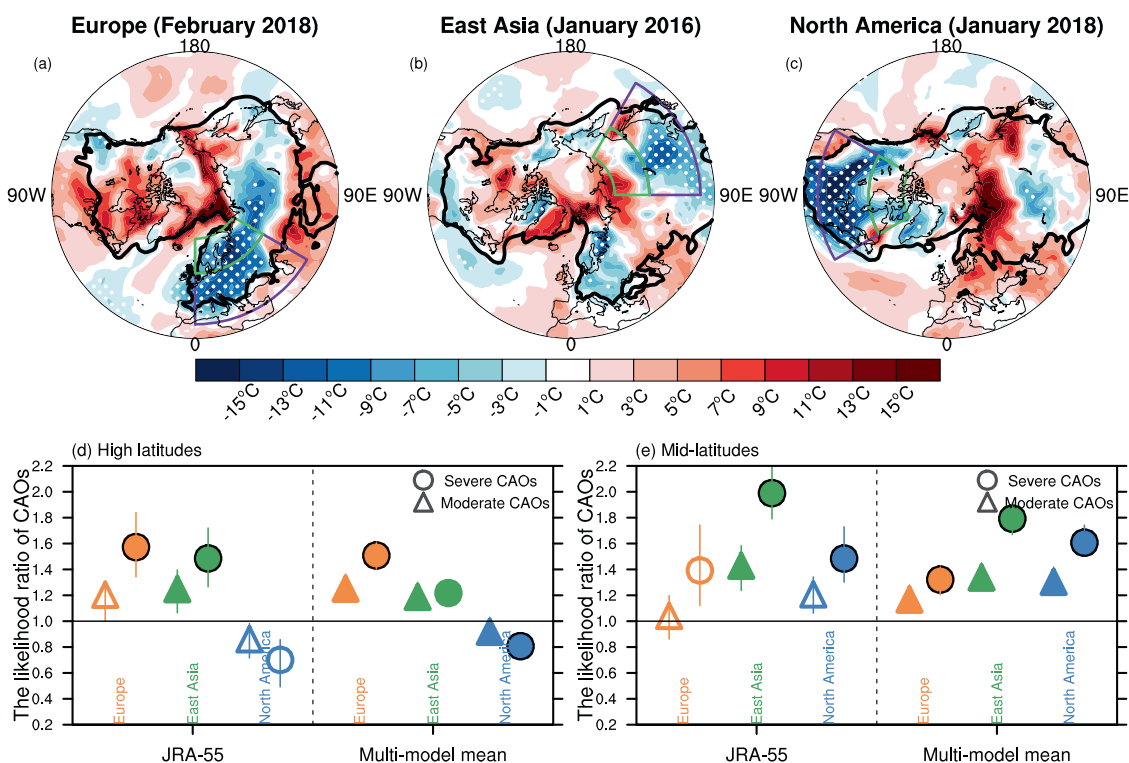


**Fig. 1** Three widely reported CAOs in recent years and the risk of CAOs. **a–c** Anomaly of surface air temperature on 27 February 2018, 22 January 2016, and 1 January 2018 when a severe CAO occurred in Europe, East Asia, and North America, respectively. According to previous studies<sup>61,62</sup>, the occurrences of European CAO and East Asian CAO are influenced by the polar vortex weakening. Stippled regions indicate that the anomalies are  $\pm 1.2$  times lower than the local standard deviation of SAT anomaly and show which regions could be defined as severe in this study. Green (purple) boxes represent the high-latitude (mid-latitude) regions in this study. The thick black solid contours indicate zero isotherms. **d** The simultaneous likelihood ratio of severe CAOs (circle) and moderate CAOs (triangle) over high-latitude Europe (in orange), East Asia (in green), and North America (in blue) under weak polar vortex conditions for the reanalysis dataset (left column) and the multi-model mean (right column). **e** As shown in **(d)**, but for the likelihood ratio in mid-latitudes. The filled markers denote that the likelihood is statistically significant and the circles with a black outline indicate that the differences between the risk of severe and moderate CAOs are statistically significant with a 95% confidence level based on 1000-time bootstrap samples with replacement. The error bars denote 95% confidence intervals estimated by 1000-time bootstrap samples with replacement.

precursors of tropospheric weather and climate anomalies than those in the middle and upper stratosphere<sup>20,28</sup>. As shown in Fig. 1, we have normalized the simultaneous occurrence of CAOs by their climatological occurrence frequency (see Supplementary Tables 1 and 2). A value of 1 thus implies no statistical relationship between a weak polar vortex and CAOs. Over Europe, the occurrence of severe CAOs in high latitudes increases by 60% under weak polar vortex conditions (Fig. 1d); this is three times larger than the concurrent increase in moderate CAOs in European high latitudes (~20%). There is a 50% increase in the occurrence of severe CAOs in high-latitude East Asia, which is larger than the increase in moderate CAOs (~25%) under weak polar vortex conditions. In the mid-latitudes of East Asia, the occurrence of severe CAOs increases by 100% under weak polar vortex conditions; this is more than two times larger than the increase in moderate CAOs (40%). The only region considered which shows a decrease in both severe and moderate CAOs under weak polar vortex conditions is North American high latitudes. In North American mid-latitudes, the occurrence of severe CAOs increases by 50% under weak polar vortex conditions, whereas the increase is only ~20% for moderate CAOs. We also evaluate the probability that there is at least one severe CAO day within 30 days following a weak polar vortex. We find that over multiple regions of the northern extratropics, except for North America, this probability is close to 1. Considering the larger societal impacts of severe CAOs, the presence of a weak polar vortex is thus associated with a disproportionate increase in the risk of fatalities, travel disruption, and economic losses. Indeed a recent study has found increased mortality in the UK linked to sudden stratospheric warmings (SSWs)<sup>29</sup>. The present results show the impacts are felt more broadly across the Northern Hemisphere.

To verify our findings, we analyze the preindustrial control simulations from a subset of climate models participating in the Coupled Model Intercomparison Project Phase 6 (CMIP6, see Supplementary Table 3 for the list of models). The multi-model mean successfully reproduces the overall response of CAOs to weak polar vortex conditions (Fig. 1d, e). In particular, the models capture a larger increase in the occurrence of severe CAOs over high latitudes of Europe (Fig. 1d) and mid-latitudes of North America and East Asia (Fig. 1e), as compared to moderate CAOs, supporting the result from the reanalysis dataset of the increased likelihood of severe CAOs in multiple regions of the northern extratropics under weak polar vortex conditions.

Considering the long persistence of lower stratospheric temperature and circulation anomalies during winter<sup>12,14</sup>, we calculate the likelihood ratio of CAOs as a function of the time lag between the polar vortex state and CAOs (see “Methods”). Negative lags in Fig. 2 denote that the occurrence of CAOs leads the weakening of the polar vortex, indicative of tropospheric precursors to the stratospheric anomalies<sup>16</sup>, whereas positive lags denote that the polar vortex anomaly leads the occurrence of CAOs and thus imply that the polar vortex provides predictive information for the occurrence of CAOs. Overall, in both the reanalysis data (Fig. 2a, b) and the CMIP6 multi-model mean (Fig. 2c, d), the risk of severe CAOs is significantly and substantially elevated relative to that of moderate CAOs in multiple regions of the northern extratropics at positive lags of up to two months, highlighting the predictive value of the weak polar vortex states.

Over high latitudes of Europe, the enhanced likelihood of severe CAOs under weak polar vortex conditions remains statistically significant and larger than for moderate CAOs at a time lag beyond one month in the reanalysis dataset (Fig. 2a). The maximum increase in the likelihood of severe CAOs in this region (65%) occurs 3 weeks after the onset of a weak polar vortex. The CMIP6 multi-model mean shows similar behavior, but the increased

occurrence of severe CAOs lasts for nearly 2 months (Fig. 2c), in part due to the longer period of the model simulations. In contrast, according to the reanalysis data, the occurrence of severe CAOs over mid-latitude Europe is unchanged following weak polar vortex conditions (Fig. 2b); this is consistent with previous studies that have reported colder surface air temperature anomalies over northern Europe than over southern Europe following SSWs<sup>30</sup>.

Over high-latitude East Asia, a weak polar vortex significantly increases the occurrence of severe and moderate CAOs (Fig. 2a) at a lead time of 20 days and 40 days, respectively, with increases in the occurrence of severe CAOs larger than that of moderate CAOs. The multi-model mean similarly shows an enhanced occurrence of severe and moderate CAOs after 2 weeks following the polar vortex anomalies (Fig. 2c). Interestingly, the occurrence of severe CAOs shows a fluctuating behavior after a weak polar vortex, with a decreased occurrence over the first 2 weeks and an increased occurrence 2 weeks following the polar vortex anomalies (Fig. 2c). The decreased occurrence is likely associated with transient warming over East Asia that has been observed to follow SSWs<sup>31</sup> (e.g., there is a transient decrease in the anomalous cold air mass flux towards high-latitude East Asia over the first 2 weeks following the polar vortex anomalies, please refer to the analysis of physical mechanism later).

Over mid-latitude East Asia, the increase in the likelihood of severe CAOs under weak polar vortex conditions is the largest among the three mid-latitude regions. The increased occurrence of severe CAOs is also significantly larger than that of moderate CAOs, with a maximum difference at a time lag of 2 days (Fig. 2b, d). The enhancement in the likelihood of severe CAOs over mid-latitude East Asia is strongly peaked, dropping rapidly over the week following weak polar vortex conditions. Interestingly, both the reanalysis and models show a significantly enhanced occurrence of severe CAOs over mid-latitude East Asia prior to a weakening of the polar vortex; this suggests that there could exist a common cause of a weak polar vortex and severe CAOs, such as Ural blocking<sup>10,32</sup>. We further analyze Ural blocking (see Supplementary Methods for definition) before and after a weak polar vortex. The occurrence likelihood of Ural blocking is enhanced before weak polar vortex conditions but decreases rapidly after the polar vortex weakening (Supplementary Fig. 1a). In addition, the positive geopotential height anomalies over the Ural Mountains significantly weaken following weak polar vortex days (compare Supplementary Fig. 2a with Supplementary Fig. 2d). This suggests that Ural blocking may be a precursor to the polar vortex weakening<sup>33–35</sup> and leads to an increased occurrence of severe CAOs over East Asia<sup>10,32</sup> prior to weak polar vortex conditions. However, it cannot explain the increased occurrence of severe CAOs following the polar vortex weakening.

The occurrence of severe CAOs over high-latitude North America decreases following a weak polar vortex, with a maximum reduction at a time lag of 10 days, according to both reanalysis and models (Fig. 2a, c). A reduction in CAO occurrence in this region is consistent with significant warm anomalies over eastern Canada following SSWs<sup>13,16</sup>. The enhanced likelihood of severe CAOs over mid-latitude North America under weak polar vortex conditions (Fig. 2b, d) only persists for five days following the polar vortex anomalies.

Overall, we find that weak polar vortex conditions substantially increase the risk of severe CAOs as compared to moderate CAOs, with a timeframe extending from synoptic to subseasonal timescales. The results highlight that the impact of the polar vortex on the severity of CAOs is not homogeneous, and that the most severe CAOs are disproportionately influenced. Our results are not sensitive to shifts in the geographical definition of the regions considered (Supplementary Fig. 3), or to the thresholds used to define CAOs (Supplementary Figs. 4 and 5).

## Likelihood of CAOs under weak polar vortex conditions

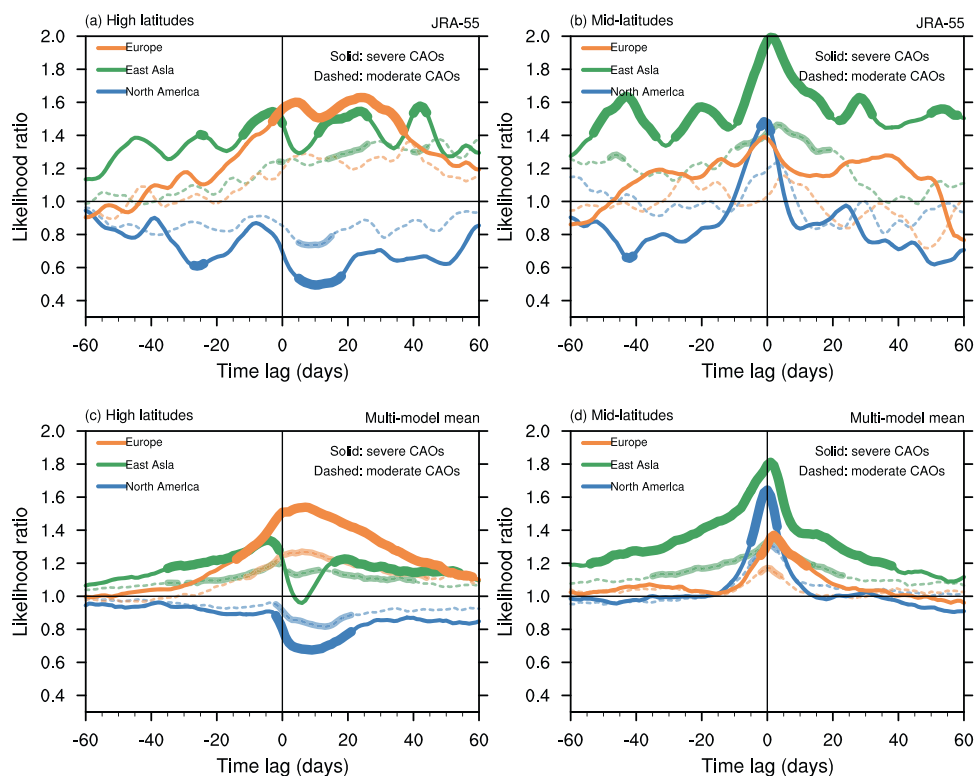


**Fig. 2** The time-lagged likelihood of CAOs under weak polar vortex conditions. **a** The likelihood of severe CAOs (solid lines) and moderate CAOs (dashed lines) in high latitudes under weak polar vortex conditions as a function of the lag between the polar vortex state and the CAOs for the reanalysis data. For instance, a lag of 20 days indicates that the likelihood of CAOs is conditional upon the weak polar vortex 20 days before (see Methods). Shown is a 5-day running mean of the likelihood of CAOs to remove the noise in the reanalysis data. Note that the main conclusions are not sensitive to the smoothing. The blue, orange, and green curves respectively represent North America, Europe, and East Asia. **b** As shown in **(a)**, but for mid-latitude regions. **c, d** As shown in **(a)** and **(b)**, respectively, but for the results of the multi-model mean. The thick line segments indicate that both the likelihood of CAOs and their difference between severe and moderate CAOs are statistically significant at a 95% confidence level. The significance is estimated by the bootstrap resampling method of repeating 1000-time random selections with replacement.

### Comparison with the relationship between the AO and CAOs.

Studies have shown that the Arctic Oscillation (AO) or North Atlantic Oscillation (NAO) also affects the occurrence of CAOs in the northern extratropics<sup>36–39</sup>. Hereafter, we analyze the AO, but similar results are obtained from the NAO. It is also well established that the weak polar vortex often leads to a negative AO phase<sup>7,40</sup> (see Supplementary Fig. 2c, d). A natural hypothesis, then, is that the effect of a weakened polar vortex on the occurrence of severe CAOs may arise through its influence on the AO.

Supplementary Fig. 6 confirms that negative AO conditions indeed increase the likelihood of severe CAOs over most regions of the northern extratropics. Particularly, the likelihood of severe CAOs over high-latitude Europe is larger under negative AO conditions than under weak polar vortex conditions within a lead time of 2 weeks (compare Fig. 2 with Supplementary Fig. 6), increasing by 140% under negative AO conditions at a lead time of 5 days. The weak polar vortex indeed shifts the frequency of the AO index toward more extreme negative values (Supplementary Fig. 7a) and increases the occurrence of extremely negative AO events (Supplementary Fig. 7b). However, the differences in the regional features of the time-lagged occurrence of severe CAOs under weak polar vortex and negative AO conditions (Fig. 2 and Supplementary Fig. 6) suggest the impact of the weakened polar vortex on severe CAOs cannot be explained simply by the AO response.

To support this point, Fig. 3 shows the frequency distribution of CAOs as a function of the temperature threshold used to define them (i.e.,  $\alpha$  in Eq. (1), see “Methods”) for all winter days, for weak polar vortex days, and for negative AO days. The thresholds used to designate moderate and severe CAOs are indicated by the cyan and blue shading, respectively. If the influence of the weak polar vortex on CAO occurrence arises exclusively through an influence on the AO, then the response of CAOs in each region of the northern extratropics to the weak polar vortex should be proportional to the associated change in the AO index (Supplementary Fig. 7a).

Over high-latitude Europe (Fig. 3a), the frequency distribution shifts significantly ( $p < 0.01$ , using a two-sample Kolmogorov–Smirnov test) more toward severe CAOs under negative AO conditions than under weak polar vortex conditions. In midlatitudes of North America (Fig. 3b), the frequency distribution under weak polar vortex conditions is the same as that under negative AO conditions. In midlatitudes of East Asia (Fig. 3c) the frequency distribution shifts more toward the severe CAO threshold under weak polar vortex conditions than under negative AO conditions ( $p < 0.01$ ). These regional differences confirm an important role of the AO for the weakened polar vortex impacting on severe CAOs over Europe, but also suggest that other potential physical processes should be considered when analyzing the impact of a weakened polar vortex on severe CAOs

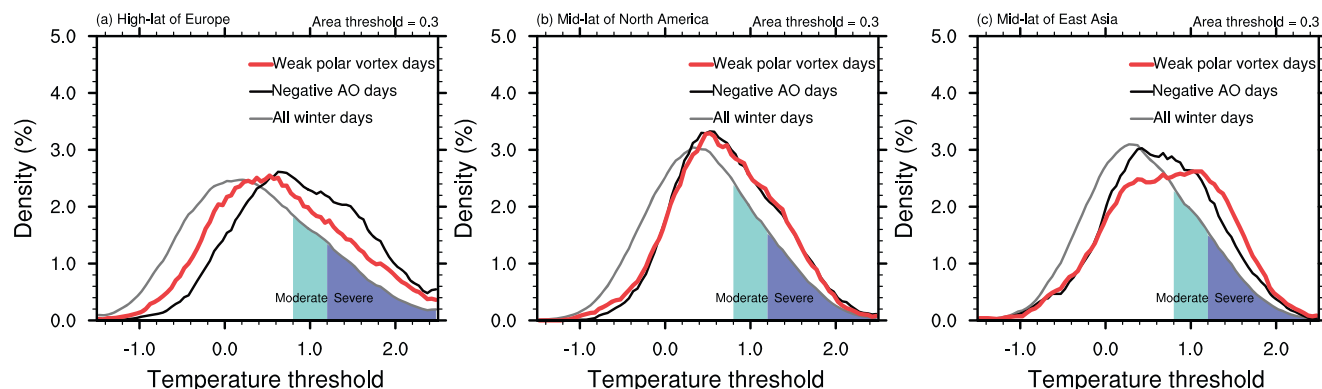


**Fig. 3** Comparisons between the effects of the weak polar vortex and the negative AO on CAOs. **a** The frequency distribution of CAOs as a function of the temperature threshold used to define CAOs under all winter days (in gray), under weak polar vortex days (in red), and under negative AO days (in black) for the reanalysis dataset. **b, c** As shown in **(a)**, but for mid-latitudes of North America and East Asia, respectively. Cyan and blue shading respectively indicate the range of thresholds used to define the moderate and severe CAOs.

over other regions, especially over East Asia. A similar analysis of the multi-model mean (Supplementary Fig. 8) and of other regions (Supplementary Fig. 9) further supports this suggestion.

**Physical mechanisms and Granger causality.** Several mechanisms have been proposed to explain the impact of a weakened polar vortex on the troposphere, such as the tropospheric response to stratospheric potential vorticity anomalies<sup>41,42</sup>, a stratospheric reflection of upward-propagating planetary waves<sup>43,44</sup>, stratospheric influence on baroclinic instability<sup>45</sup> and on circulation regimes<sup>46</sup>. These physical mechanisms explain the stratospheric influence on the troposphere in some cases but are still under investigation. Considering that severe CAOs are often related to anomalous cold air mass amounts, we hypothesize that a weakened polar vortex affects severe CAOs by impacting the transport of cold air mass.

To test this hypothesis, we analyze the cold air mass amount and its flux, following the method of Iwasaki et al.<sup>47</sup>, before and after weak polar vortex conditions (Fig. 4). Climatologically, there are two main cold air mass streams that bring cold Arctic air masses to the midlatitudes: The East Asian stream and the North American stream (Supplementary Fig. 10). The East Asian stream grows over the Eurasian continent and flows eastward, and the North American stream grows over the Arctic Ocean, flows across the Arctic and toward the eastern coast of North America. Following a weakening of the polar vortex, the North American cold stream weakens (compare Fig. 4a with Fig. 4d), with the anomalous cold air mass flowing westward opposite to the climatological state. The weakening of the North American cold stream leads to a weak inter-hemispheric transport of polar cold air mass (PCAM) from the Eastern Hemisphere to the Western Hemisphere. Consequently, there is less cold air mass flowing toward high latitudes of North America and more cold air mass accumulating over the Eurasian continent. This explains the decrease in the likelihood of severe CAOs over high latitudes of North America and the increase in the likelihood of severe CAOs over Eurasia (Fig. 2). This also explains why the likelihood of severe CAOs over mid-latitude North America is only increased around Day 0 (Fig. 2b): there is initially an increase in cold air mass transport into the midlatitudes, but the high-latitude source for this excess is rapidly depleted, due to the reduced inter-hemispheric transport over the Arctic.

Previous studies<sup>48–51</sup> have stressed the importance of the meridional transport of cold air mass. They<sup>48–51</sup> stated that a stronger warm-air branch into the upper polar atmosphere is synchronized with a stronger equatorward cold-air branch in

lower levels, responsible for anomalous cold conditions in midlatitudes and anomalous warm conditions in high latitudes. The present emphasis on changes in inter-hemispheric cold air mass transport clarifies the regional differences in the timing of CAOs following weak vortex conditions, a feature which is not easily explained from the perspective of meridional circulations or from the anomalous state of the AO.

To further support this hypothesis, we define an index describing the inter-hemispheric cold air mass transport from the Eastern Hemisphere to the Western Hemisphere (see “Methods” for the definition). Figure 4e shows the time-lagged composite of anomalous inter-hemispheric cold air mass transport under weak polar vortex and negative AO conditions. Both weak polar vortex and negative AO conditions significantly weaken the inter-hemispheric cold air mass transport, but there are important differences between the composited anomalies. The decrease in inter-hemispheric cold air mass transport persists for more than 3 weeks following the polar vortex anomalies. However, the decrease in inter-hemispheric cold air mass transport is strongly peaked, dropping rapidly over 5 days following negative AO conditions. This suggests that the polar vortex can affect the inter-hemispheric cold air mass transport at a longer lead time. The differences in the spatial patterns of cold air mass amount and its flux under weak polar vortex and negative AO conditions further support this suggestion (compare Supplementary Fig. 11d and Fig. 4d). In addition, we define weak inter-hemispheric cold air mass transport days (see Methods) and calculate the likelihood of them under weak polar vortex and negative AO conditions. The result shows that the enhanced likelihood of weakened inter-hemispheric cold air mass transport persists longer following a weakened polar vortex than following a negative AO phase (Fig. 4f), supporting that the polar vortex states give predictive power to the extended-range forecast of severe CAOs.

To evaluate the predictive power given by the polar vortex to the forecast of severe CAOs and the relevance of the inter-hemispheric cold air mass transport to the linkage between the weakened polar vortex and severe CAOs, we apply a novel method that assesses Granger causality using logistic regression<sup>52</sup> to evaluate the probabilistic forecast skill for severe CAOs. We first estimate two logistic models: The reference model and the polar vortex (POV) model. The reference model only includes the past state of CAOs as predictors, while the POV model includes past states of the polar vortex. We can assess directly whether the polar vortex provides predictive information regarding severe CAOs by comparing the performance of the reference model and

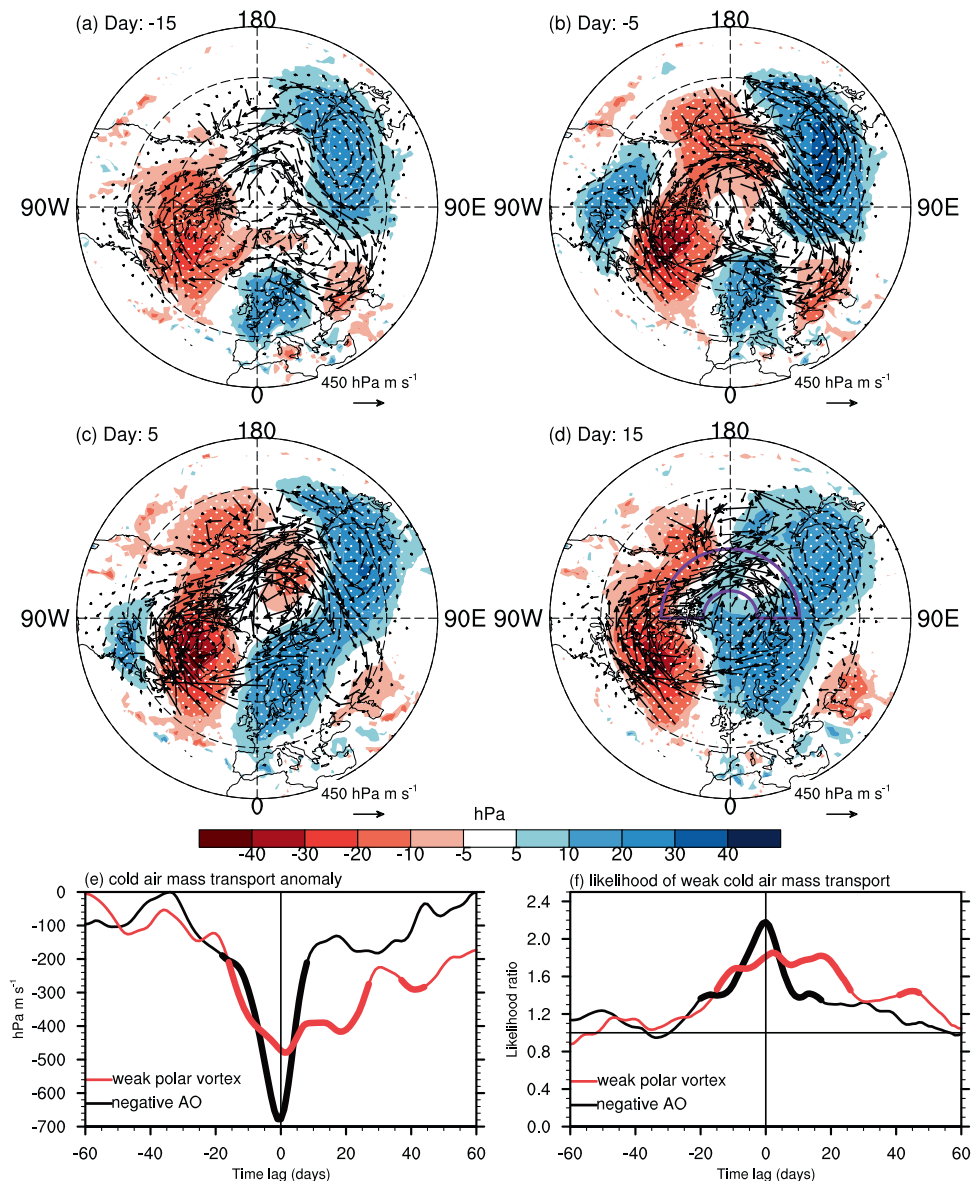


**Fig. 4 The weakened inter-hemispheric transport of cold air mass related to a weak polar vortex.** The composited geographical distributions of the anomalous cold air mass amount (shading; hPa) below the 280 K isentropic surface and their horizontal flux (arrows;  $\text{hPa m s}^{-1}$ ) 15 days before (a), 5 days before (b), 5 days after (c), and 15 days after (d) weak polar vortex conditions obtained from the JRA-55 reanalysis dataset. Stippling indicates that the anomalies are statistically significant at a 95% confidence level based on a two-sided Student's *t* test. The purple box in (d) indicates the area used to calculate the inter-hemispheric transport of cold air mass. Note that cold color means anomalous high cold air mass and warm color means anomalous low cold air mass. **e** The time-lagged composite of anomalous inter-hemispheric cold air mass transport under weak polar vortex (red curve) and negative AO (black curve) conditions. The inter-hemispheric cold air mass transport has a climatological value of  $-350 \text{ hPa m s}^{-1}$ . **f** The time-lagged likelihood of the weakened inter-hemispheric cold air mass transport under weak polar vortex (red curve) and negative AO (black curve) conditions. The definitions of positive and negative lags are the same as shown in Fig. 2. The thick line segments in (e) and (f) indicate that the composited anomaly and the likelihood, respectively, are statistically significant at a 95% confidence level based on 1000-time bootstrap samples with replacement.

the POV model. Then we estimate two logistic models: The combined model and the PCAM model. The combined model includes past states of inter-hemispheric cold air mass transport on the basis of the POV model. However, in the PCAM model, we apply past states of the polar vortex to evaluate the forecast skill for the weakened inter-hemispheric cold air mass transport, rather than the forecast skill for severe CAOs. We can examine the proposed mechanism by assessing the significant links among a weak polar vortex, a weakened cold air mass transport, and severe CAOs (see Methods for full details).

The results are summarized graphically in Fig. 5. In this diagram, the squares indicate the state of the polar vortex or the

cold air mass transport (predictors) and the circles indicate the occurrence of CAOs in specific regions of interest (predictands). Note that in the PCAM model the state of cold air mass transport is also used as the predictand. An arrow drawn from a predictor to a predictand indicates that the predictor provides predictive information, with dashed arrows denoting that the predictor 6–10 days before provides predictive information to the predictand and solid arrows for the predictor 1–5 days before. Where such a link exists, the arrow colors represent the strength of the causal links as quantified by the regression coefficient.

According to the reanalysis data (Fig. 5a), the polar vortex itself provides predictive information regarding severe CAOs over all

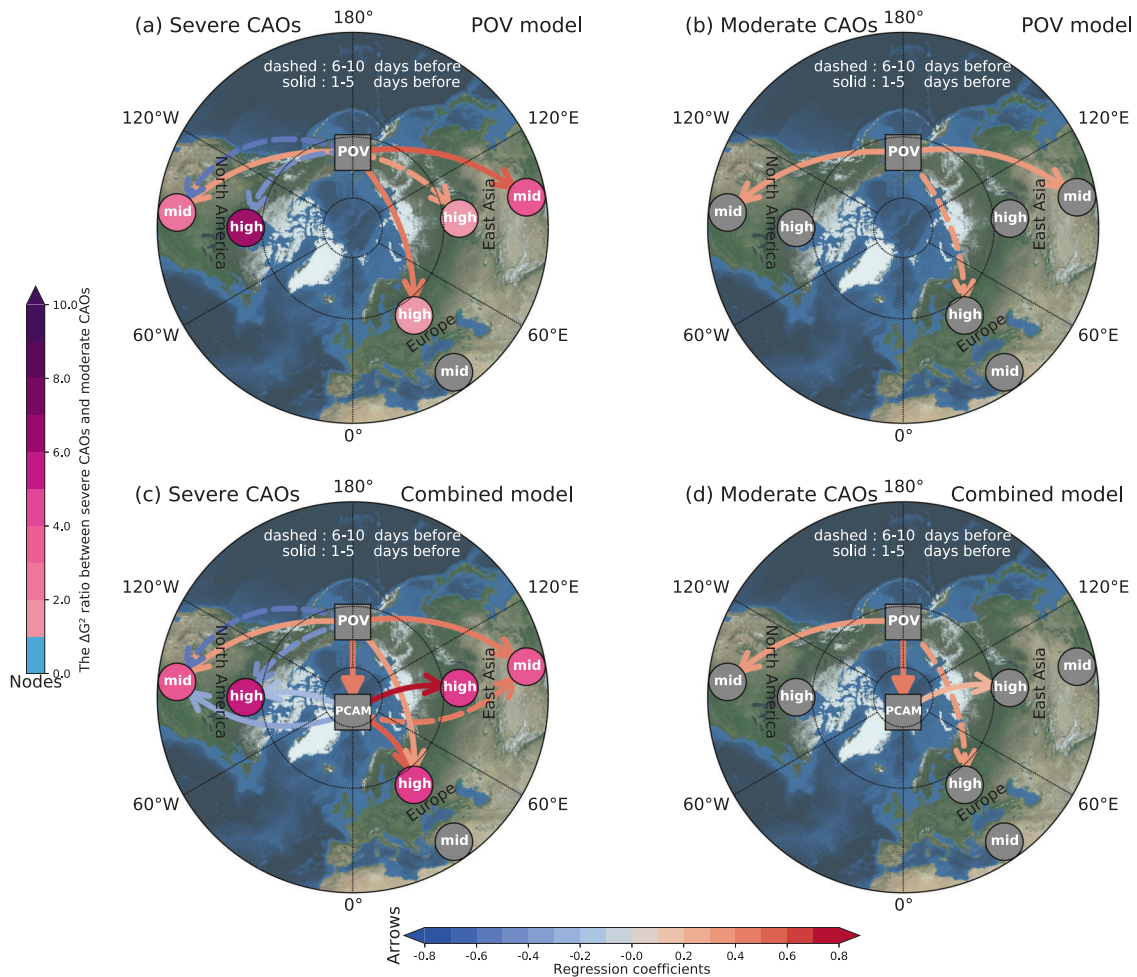


**Fig. 5 Graphical representation of Granger causality using logistic regression.** **a** The results of Granger causality analysis of severe CAOs in terms of the POV model according to the reanalysis data. **b** As shown in **(a)**, but for moderate CAOs. **c, d** As shown in **(a)** and **(b)**, respectively, but for the Granger causality analysis in terms of the combined model. Note that we add the significant links between the polar vortex and the cold air mass transport in **(c)** and **(d)**, respectively. Circles represent the predictands, namely, the current states of CAOs at high latitudes and mid-latitudes. Squares denote predictors (e.g., POV or PCAM), namely, past states of the polar vortex and the cold air mass transport. The arrows denote the direction of the influence, with dashed arrows denoting that the predictor 6–10 days before provides predictive information to the predictand and solid arrows for the predictor 1–5 days before. The arrow colors denote the logistic regression coefficients with only statistically significant links ( $p < 0.05$ ) being presented (the color bar on the bottom; the contour interval is 0.1). The node colors in **(a)** and **(c)** indicate the ratio between the  $\Delta G^2$  of severe CAOs and that of moderate CAOs (the color bar to the left; the contour interval is 1.0). A larger value of  $\Delta G^2$  means a better model performance. See “Methods” for the definition of  $\Delta G^2$ . We do not color the node over mid-latitude Europe, since there is not a significant link for both severe and moderate CAOs.

high-latitude regions and mid-latitudes of East Asia and North America. The CMIP6 multi-model mean is consistent with these findings; in particular, the multi-model mean successfully captures the significant causal links (Supplementary Fig. 12) seen in the reanalysis dataset. We find that the polar vortex has a positive effect on the inter-hemispheric cold air mass transport (Fig. 5c). Thus, a weak polar vortex can lead to a weakened inter-hemispheric cold air mass transport. We also find positive links between the cold air mass transport and severe CAOs over Eurasia and negative links between the cold air mass transport and severe CAOs over North America, which means that a weakened inter-hemispheric cold air mass transport favors an increased occurrence of severe CAOs over Eurasia and a decreased occurrence over North America. There are other direct links between the polar vortex and severe CAOs, suggesting that there exist other processes responsible for the polar vortex impacting severe CAOs. For instance, the increased occurrence of severe CAOs over mid-latitude North America is likely related to the

effect of the polar vortex on Alaskan blocking<sup>18</sup> (see Supplementary Fig. 1b).

Comparing the causal links of severe CAOs (Fig. 5a, c) with that of moderate CAOs (Fig. 5b, d), we find that there are few significant causal links of moderate CAOs. Furthermore, we calculate the likelihood ratio statistics ( $\Delta G^2$ ; see “Methods”) to evaluate the performance of the POV model relative to the reference model; here a larger value indicates an improvement in the model performance after including the polar vortex state. The node colors depict the ratio between the  $\Delta G^2$  of severe CAOs and that of moderate CAOs. We find that the influence of a weak polar vortex has a more pronounced impact on the predictability of severe CAOs than on moderate CAOs.

### Conclusions and discussions

Through a combination of reanalysis data and state-of-the-art climate models, we provide corroborative evidence that weak polar vortex conditions in the lower stratosphere substantially

increase the risk of severe CAOs over most continental regions of the northern extratropics. The increase in the risk of severe CAOs is disproportionate as compared to moderate CAOs. This is particularly notable over mid-latitude East Asia, where severe CAOs are up to twice as likely to occur following weak polar vortex conditions, in contrast to moderate CAOs which are only 40% more likely to occur. The elevated risk of severe CAOs over high-latitude Europe, high-latitude East Asia (with a lag of 2 weeks), and mid-latitude East Asia typically last for more than 3 weeks following polar vortex anomalies. There is also an elevated risk of severe CAOs in the mid-latitudes of North America, but unlike in the other regions just mentioned, this does not persist beyond about five days following weak polar vortex anomalies. Further analysis confirms the existence of a dynamical pathway by which the polar vortex affects severe CAOs that is distinct from its influence on the AO, especially over East Asia. By analyzing the cold air mass stream, we find that the weak polar vortex affects severe CAOs of the northern extratropics by weakening the inter-hemispheric transport of cold air mass from the Eastern Hemisphere to the Western Hemisphere. Using a novel method to assess Granger causality, we further show that the polar vortex state provides predictive information regarding severe CAOs over most regions of the northern extratropics and verify the proposed mechanism.

By comparing the predictive power to the forecast of severe CAOs given by the inter-hemispheric cold air mass transport with that given by the AO, we find that the cold air mass transport gives additional information to the forecast of severe CAOs over North America and East Asia that is independent of predictive information arising from the AO (see Supplementary Methods and Supplementary Fig. 13). This supports the importance of the inter-hemispheric cold air mass transport pathway in understanding the influence of the stratospheric polar vortex on severe CAOs. Further study is needed to clarify how the polar vortex affects inter-hemispheric cold air mass transport.

Our results have implications for skillful sub-seasonal forecasts and successful mitigation of the impacts of severe CAOs. This novel approach of Granger-causality analysis can be directly applied to operational subseasonal and seasonal forecast models to assess and improve their ability to exploit the predictive skill related to the stratospheric polar vortex.

**Methods**

**Datasets.** The Japanese 55-year Reanalysis (JRA-55) dataset<sup>53</sup> for the period 1958–2019 is used in this study. While reanalysis datasets in the pre-satellite era have larger uncertainties in their representation of stratospheric conditions, for examining extremes such as SSWs the improved statistics from the increased sample size generally outweighs the impacts of the larger uncertainty from the reanalysis fields<sup>54</sup>. We also use the preindustrial control simulations from 11 CMIP6 models to verify the results of the reanalysis data. 7 out of 11 are high-top models (i.e., a model top is at or above 0.1 hPa), and the choice of models follows that of ref. <sup>55</sup>. The models and the length of control simulation used are listed in Supplementary Table 3, and see Table 1 in ref. <sup>55</sup>. for more details about these models.

**The definition of CAOs.** We use established indices<sup>51</sup> to identify CAOs in high-latitude (55°–70°N) and mid-latitude (35°–55°N) regions of Europe (0°–60°E), East Asia (90°–150°E) and North America (120°–60°W). For a given dataset of surface air temperature (SAT) fields, the climatology is calculated by averaging the daily SAT field at each grid point across all available years of the daily SAT dataset for each calendar day from 1 November to 31 March. The anomalies presented in this paper are obtained by subtracting the daily climatological annual cycle from the original data at all time steps, and the linear trend of the anomalies (if it exists) has been removed. The CAO index (referred to as *area threshold*) is calculated as follows:

$$CAO_{index} = \frac{\int_{\varphi_S}^{\varphi_N} \int_{\lambda_W}^{\lambda_E} H(-\alpha \times LSD - SAT') a \cos \varphi d\lambda d\varphi}{\int_{\varphi_S}^{\varphi_N} \int_{\lambda_W}^{\lambda_E} a \cos \varphi d\lambda d\varphi} \tag{1}$$

where LSD is the local standard deviation of SAT anomaly fields (SAT'), *a* is the

radius of the Earth, and *H(x)* is the Heaviside function, such that *H(x)* = 1 for *x* > 0 and otherwise *H(x)* = 0. The index measures the percentage area occupied by cold SAT anomalies below  $-\alpha \times LSD$ . A large value of CAO index corresponds to CAOs with broader spatial coverage. Here,  $\alpha$  sets the temperature threshold used to identify a CAO, where a large value of  $\alpha$  requires CAOs to have a lower SAT.

CAOs are defined in terms of both temperature and area threshold. We use an area threshold of 30% (i.e., 30% of the region must be anomalously cold). Moderate CAOs are defined by a temperature threshold between 0.8 and 1.2, while the threshold for severe CAOs is 1.2 (i.e., SAT anomaly is lower than  $-1.2$  times LSD). The total number of CAOs and their climatological frequency for high latitudes and midlatitudes are shown in Supplementary Tables 1 and 2, respectively. To have a direct sense of the severity of CAOs, we show the SAT anomaly area-averaged over each of these selected regions in Supplementary Table 4, which corresponds to the temperature thresholds defining CAOs.

Another type of severe CAO can be defined by keeping the temperature threshold constant (i.e., 0.4) and requiring an area threshold larger than the value of 65%. For moderate CAOs, we have an area threshold between 50% and 65%. This type of severe CAOs has wider spatial coverage.

**The weak polar vortex and negative AO days.** Several methods have been proposed to define major Sudden Stratospheric Warmings<sup>56</sup> (SSWs), most of them being based on the state of the polar vortex at 10 hPa or 50 hPa. However, these definitions in the middle and upper stratosphere mainly focus on the stratosphere itself. Previous studies also identified the importance of the depth to which the SSWs descend in the stratosphere, with those that penetrate to the lower stratosphere leading to the most robust tropospheric response at long time scales<sup>12,14,57</sup>. We thus define the weak polar vortex days in the lower stratosphere by requiring the lower-stratospheric daily zonal mean zonal wind anomalies at 100 hPa and 60°N to be below the overall wintertime (1 November to 31 March) 15th percentile<sup>58</sup>. The daily AO index is defined as the principal component time series of the leading Empirical Orthogonal Function of daily sea level pressure anomalies poleward of 20°N in the North Hemisphere<sup>59</sup>. We define extreme negative AO days by requiring the AO index to be below the overall wintertime 15th percentile. According to our method, 1381 out of 9211 days (with 29 February discarded) across 61 winters are defined as weak polar vortex days in the JRA-55 reanalysis dataset. The total number of negative AO days is similar to that of weak polar vortex days.

**The inter-hemispheric transport of cold air mass.** We apply the same definition formulas as Iwasaki et al.<sup>47</sup> to calculate the cold air mass and its flux in isentropic coordinates. The cold air mass amount is calculated as follows:

$$DP = p_S - p(\theta_T) \tag{2}$$

and the *u*-component of cold air mass flux is calculated as follows:

$$u_{flux} = \int_{p(\theta_T)}^{p_S} u dp \tag{3}$$

where *p<sub>s</sub>* is surface pressure, *p*( $\theta_T$ ) is the pressure on 280 K isentropic surface, and *u* is the zonal wind in isentropic coordinates.

We further define an index describing the inter-hemispheric transport of polar cold air mass (PCAM) from the Eastern Hemisphere to the Western Hemisphere as follows:

$$PCAM_{index} = \frac{\int_{65^{\circ}N}^{80^{\circ}N} \int_{90^{\circ}E}^{90^{\circ}W} u_{flux} a \cos \varphi d\lambda d\varphi}{\int_{65^{\circ}N}^{80^{\circ}N} \int_{90^{\circ}E}^{90^{\circ}W} a \cos \varphi d\lambda d\varphi} \tag{4}$$

Where *u<sub>flux</sub>* is the *u*-component of cold air mass flux, and *a* is the radius of the earth. We define the weakened inter-hemispheric transport of cold air mass by requiring the cold air mass index to be below the overall wintertime 15th percentile.

**The risks of CAOs under weak polar vortex and negative AO conditions.** We define the risk of CAOs under weak polar vortex conditions as the conditional probability of CAOs under weak polar vortex conditions. The risk of CAOs under weak polar vortex conditions at different time lags is calculated as follows:

$$P(CAOs|POV)_{lag=l} = \frac{N_{CAOs\&POV}(l)}{N_{POV}(l)}; l = -60, -59, \dots, 0, \dots, 59, 60. \tag{5}$$

where *N<sub>POV</sub>(l)* is the total number of the weak polar vortex days during all winters at lag = *l*, and *N<sub>CAOs&POV</sub>(l)* is the total number of CAO days during all weak polar vortex days at lag = *l*. Here, *l* represents the lead-lag time, where positive *l* means that the weak polar vortex leads CAOs, and vice versa for negative *l*. To easily compare the likelihoods in terms of different thresholds and regions, we divide the likelihood of CAOs under weak polar vortex conditions by the overall likelihood of CAOs, which is calculated as follows:

$$P(CAOs)_{lag=l} = \frac{N_{CAOs}(l)}{N_{winter}(l)}; l = -60, -59, \dots, 0, \dots, 59, 60. \tag{6}$$

Here,  $N_{\text{winter}}(l)$  is the total number of all winter days at lag =  $l$ , and  $N_{\text{CAOs}}(l)$  is the total number of CAO days at lag =  $l$ .

Take  $l = 1$  as an example. Considering that the weak polar vortex days on 31 March cannot contribute to  $P(\text{CAOs} | \text{POV})_{\text{lag}=1}$  since only the period 1 November–31 March is analyzed, we thus calculate  $N_{\text{POV}}(l = 1)$  as the difference between  $N_{\text{POV}}(l = 0)$  and the total number of weak polar vortex days on 31 March during all winters. Similarly, the CAO days on 1 November cannot contribute to  $P(\text{CAOs} | \text{POV})_{\text{lag}=1}$ , since we do not consider if there was a weak polar vortex day on the previous day.  $N_{\text{CAOs}}(l = 1)$  is calculated as the difference between  $N_{\text{CAOs}}(l = 0)$  and the total number of CAO days on 1 November during all winters. Then we can count  $N_{\text{CAOs}\&\text{POV}}(l = 1)$  after discarding all CAO days on 1 November and all weak polar vortex days on 31 March.  $N_{\text{winter}}(l = 1)$  is the difference between  $N_{\text{winter}}(l = 0)$  (i.e., all winter days) and the number of winters (e.g., 61 for the JRA-55 reanalysis data when  $l = 1$ , and  $61 \times 2$  when  $l = 2$ ). Finally, the likelihood of CAOs under weak polar vortex conditions can be calculated according to Eq. (5). The likelihood of CAOs under negative AO conditions, the likelihood of negative AO under weak polar vortex conditions, and the likelihood of the weakened inter-hemispheric cold air mass transport under both conditions are calculated in a similar way.

**Granger causality analysis using logistic regression.** We analyze the Granger causality using logistic regression<sup>52</sup>. The advantage of using logistic regression is that it allows us to compare the predictive information arising from different threshold conditions, rather than assuming a linear relationship. To our knowledge, the Granger causality analysis using logistic regression is seldomly applied to the meteorological field. First, we create new binary time series that can take two values only, namely, the values 0 or 1, to indicate whether or not a given date meets the relevant threshold (i.e., severe CAOs, moderate CAOs, a weak polar vortex, and a weakened inter-hemispheric cold air mass transport). Second, we aggregate the original binary time series to emphasize the longer timescales that characterize interactions between the stratosphere and troposphere. Specifically, we divide any given winter (150 days, thus ignoring 31 March and 29 February in leap years) into ten 5-day intervals. Third, we define the dummy variables for each of the characteristics; for instance, the dummy variable for the polar vortex takes a value of 1 if more than one day in any 5-day interval is a weak polar vortex day and 0 otherwise. Note that for the dummy variable of severe CAOs, we additionally examine whether the number of moderate CAO days is larger than that of severe CAO days for any given 5-day interval. If not, we assign a value of 1 to severe CAOs, and 0 otherwise. This ensures the two dummy variables (severe and moderate CAOs) are non-overlapping. To evaluate the predictive information provided by the polar vortex, we estimate two logistic regression models as follows.

The first, or reference model, regresses the past states of CAOs onto the current states of CAOs:

$$\log\left(\frac{\pi_{\text{CAO}}}{1 - \pi_{\text{CAO}}}\right) = \beta_0 + \beta_1 \text{CAO}_{t-1} + \varepsilon \quad (7)$$

The second, or POV model, consists of the reference model, in addition to past states of the polar vortex:

$$\log\left(\frac{\pi_{\text{CAO}}}{1 - \pi_{\text{CAO}}}\right) = \beta_0 + \beta_1 \text{CAO}_{t-1} + \beta_2 \text{POV}_{t-1} + \beta_3 \text{POV}_{t-2} + \varepsilon \quad (8)$$

To examine the proposed physical mechanism, we estimate another two logistic models as follows.

The combined model consists of the reference model, in addition to past states of both the polar vortex and the cold air mass transport:

$$\log\left(\frac{\pi_{\text{CAO}}}{1 - \pi_{\text{CAO}}}\right) = \beta_0 + \beta_1 \text{CAO}_{t-1} + \beta_2 \text{POV}_{t-1} + \beta_3 \text{POV}_{t-2} + \beta_4 \text{PCAM}_{t-1} + \beta_5 \text{PCAM}_{t-2} + \varepsilon \quad (9)$$

The “PCAM” model regresses past states of both cold air mass transport and the polar vortex onto the current states of cold air mass transport:

$$\log\left(\frac{\pi_{\text{PCAM}}}{1 - \pi_{\text{PCAM}}}\right) = \beta_0 + \beta_1 \text{PCAM}_{t-1} + \beta_2 \text{POV}_{t-1} + \beta_3 \text{POV}_{t-2} + \varepsilon \quad (10)$$

where  $\pi$  is the probability that  $\text{CAO}_t = 1$  or  $\text{PCAM}_t = 1$ , that is, that a CAO or a weakened cold air mass transport will occur in the forecast period.  $\beta_i (i = 0, \dots, 5)$  is the logistic regression coefficient to be estimated, and  $\varepsilon$  represents noise.

Subscripts  $t-1$  and  $t-2$  represent the past states of predictors 1–5 days before and 6–10 days before, respectively. For the statistical significance of individual logistic regression coefficients, we apply the Wald chi-squared statistics for these tests<sup>60</sup>.

For the overall goodness-of-fit of the logistic models, we apply the likelihood ratio tests<sup>60</sup>. Suppose two nested models are under consideration, for instance, one model (e.g., the reference model) is obtained from the other one (e.g., the POV model) by putting some of the regression coefficients to be zero (e.g.,  $\beta_2$  and  $\beta_3$ ). Now we test:

$H_0$ : the reference model is true vs.  $H_A$ : the POV model is true.

The likelihood ratio statistic is calculated as follows:

$$\Delta G^2 = G^2 \text{ from the reference model} - G^2 \text{ from the POV model} \quad (11)$$

where  $G^2$ 's are the overall goodness-of-fit statistics. A large value of  $\Delta G^2$  leads to a

small  $p$ -value, which provides evidence against the reference model in favor of the POV model, thus we can say the past states of the polar vortex contain information that helps predict CAOs above and beyond the information contained in the past states of CAOs alone.

We also examine Granger causality in terms of the original, unaggregated binary time series. We use the past state one day prior to the occurrence of CAOs to represent the predictor at lag =  $t - 1$ . To compare the results obtained from the unaggregated time series with that of the aggregated time series, we apply a 5-day time interval between lag =  $t - 1$  and lag =  $t - 2$ , namely, using the past state six days prior to CAOs to represent the predictor at lag =  $t - 2$ . The overall causal links obtained from the original, unaggregated time series are similar to those of the aggregated time series.

## Data availability

The JRA-55 reanalysis data are publicly available at <https://rda.ucar.edu/datasets/ds628.0/?hash=description#access>. The CMIP6 datasets are obtained from <https://esgf-node.llnl.gov/search/cmip6/>.

## Code availability

Fortran codes for the calculation of cold air mass and its flux in isentropic coordinates are available from [http://wind.gp.tohoku.ac.jp/isen\\_cam/tutorial.html](http://wind.gp.tohoku.ac.jp/isen_cam/tutorial.html). Figures 1–4 were made with the NCAR Command Language (Version 6.6.2) [Software], (2019). Boulder, Colorado: UCAR/NCAR/CISL/TDD. <https://doi.org/10.5065/D6WD3XH5>. Python 3.6.7 was used to generate Fig. 5. The codes that were used to generate all figures in this study are available from the corresponding authors upon reasonable request.

Received: 11 January 2021; Accepted: 23 June 2021;

Published online: 23 July 2021

## References

- Zhou, B. et al. The Great 2008 Chinese Ice Storm: its socioeconomic–ecological impact and sustainability lessons learned. *Bull. Am. Meteor. Soc.* **92**, 47–60 (2010).
- Field, C. B. et al. (eds) *Managing the Risks of Extreme Events and Disasters to Advance Climate Change Adaptation* (Cambridge University Press, 2012).
- Dixon, P. G. et al. Heat mortality versus cold mortality: a study of conflicting databases in the United States. *Bull. Am. Meteor. Soc.* **86**, 937–944 (2005).
- Europe freezes as ‘Beast from the East’ arrives. *BBC News*. <https://www.bbc.com/news/world-europe-43218229> (2018).
- Morris, S., Weaver, M. & Khomami, N. Beast from the East meets storm Emma, causing UK’s worst weather in years. *The Guardian*. <https://www.theguardian.com/uk-news/2018/mar/01/beast-from-east-storm-emma-uk-worst-weather-years> (2018).
- Inman, P., Topham, G. & Vaughan, A. Freezing weather costs UK economy £1bn a day. *The Observer* (2018).
- Baldwin, M. P. & Dunkerton, T. J. Stratospheric harbingers of anomalous weather regimes. *Science* **294**, 581–584 (2001).
- Charlton, A. J. & Polvani, L. M. A new look at stratospheric sudden warmings. Part I: climatology and modeling benchmarks. *J. Clim.* **20**, 449–469 (2007).
- Kim, B.-M. et al. Weakening of the stratospheric polar vortex by Arctic sea-ice loss. *Nat. Commun.* **5**, 4646 (2014).
- Zhang, J., Tian, W., Chipperfield, M. P., Xie, F. & Huang, J. Persistent shift of the Arctic polar vortex towards the Eurasian continent in recent decades. *Nat. Clim. Change* **6**, 1094–1099 (2016).
- Hu, D., Guan, Z., Tian, W. & Ren, R. Recent strengthening of the stratospheric Arctic vortex response to warming in the central North Pacific. *Nature Communications* **9**, 1–10 (2018).
- Hitchcock, P., Shepherd, T. G. & Manney, G. L. Statistical characterization of arctic polar-night jet oscillation events. *J. Clim.* **26**, 2096–2116 (2013).
- Hitchcock, P. & Simpson, I. R. The downward influence of stratospheric sudden warmings. *J. Atmos. Sci.* **71**, 3856–3876 (2014).
- Runde, T., Dameris, M., Garny, H. & Kinnison, D. E. Classification of stratospheric extreme events according to their downward propagation to the troposphere. *Geophys. Res. Lett.* **43**, 6665–6672 (2016).
- Zhang, R. et al. The corresponding tropospheric environments during downward-extending and nondownward-extending events of stratospheric northern annular mode anomalies. *J. Clim.* **32**, 1857–1873 (2019).
- Kolstad, E. W., Breiteig, T. & Scaife, A. A. The association between stratospheric weak polar vortex events and cold air outbreaks in the Northern Hemisphere. *Q. J. R. Meteorol. Soc.* **136**, 886–893 (2010).
- Kretschmer, M. et al. More-persistent weak stratospheric polar vortex states linked to cold extremes. *Bull. Am. Meteor. Soc.* **99**, 49–60 (2018).

18. Kretschmer, M., Cohen, J., Matthias, V., Runge, J. & Coumou, D. The different stratospheric influence on cold-extremes in Eurasia and North America. *npj Clim. Atmos. Sci.* **1**, 1–10 (2018).
19. Thompson, D. W. J., Baldwin, M. P. & Wallace, J. M. Stratospheric connection to northern hemisphere wintertime weather: implications for prediction. *J. Clim.* **15**, 1421–1428 (2002).
20. Baldwin, M. P. et al. Stratospheric memory and skill of extended-range weather forecasts. *Science* **301**, 636–640 (2003).
21. Maycock, A. C., Keeley, S. P. E., Charlton-Perez, A. J. & Doblas-Reyes, F. J. Stratospheric circulation in seasonal forecasting models: implications for seasonal prediction. *Clim. Dyn.* **36**, 309–321 (2011).
22. Sigmond, M., Scinocca, J. F., Kharin, V. V. & Shepherd, T. G. Enhanced seasonal forecast skill following stratospheric sudden warmings. *Nat. Geosci.* **6**, 98–102 (2013).
23. Domeisen, D. I. V. et al. The role of the stratosphere in subseasonal to seasonal prediction: 2. Predictability arising from stratosphere-troposphere coupling. *J. Geophys. Res.* **125**, e2019JD030923 (2020).
24. Waugh, D. W., Sobel, A. H. & Polvani, L. M. What is the polar vortex and how does it influence weather? *Bull. Am. Meteor. Soc.* **98**, 37–44 (2017).
25. Huang, J. & Tian, W. Eurasian cold air outbreaks under different arctic stratospheric polar vortex strengths. *J. Atmos. Sci.* **76**, 1245–1264 (2019).
26. Maycock, A. C. & Hitchcock, P. Do split and displacement sudden stratospheric warmings have different annular mode signatures? *Geophys. Res. Lett.* **42**, 10,943–10,951 (2015).
27. Karpechko, A. Y., Hitchcock, P., Peters, D. H. W. & Schneidereit, A. Predictability of downward propagation of major sudden stratospheric warmings. *Q. J. R. Meteorol. Soc.* **143**, 1459–1470 (2017).
28. Christiansen, B. Downward propagation and statistical forecast of the near-surface weather. *J. Geophys. Res.* **110**, D14104 (2005).
29. Charlton-Perez, A. J., Huang, W. T. K. & Lee, S. H. Impact of sudden stratospheric warmings on United Kingdom mortality. *Atmos. Sci. Lett.* **22**, e1013 (2021).
30. King, A. D., Butler, A. H., Jucker, M., Earl, N. O. & Rudeva, I. Observed relationships between sudden stratospheric warmings and European climate extremes. *J. Geophys. Res.* **124**, 13943–13961 (2019).
31. Woo, S.-H., Kim, B.-M. & Kug, J.-S. Temperature variation over East Asia during the lifecycle of weak stratospheric polar vortex. *J. Clim.* **28**, 5857–5872 (2015).
32. Tyrllis, E. et al. Ural blocking driving extreme arctic sea ice loss, cold Eurasia, and stratospheric vortex weakening in autumn and early winter 2016–2017. *J. Geophys. Res.* **124**, 11313–11329 (2019).
33. Woollings, T., Charlton-Perez, A., Ineson, S., Marshall, A. G. & Masato, G. Associations between stratospheric variability and tropospheric blocking. *J. Geophys. Res.* **115**, D06108 (2010).
34. Martius, O., Polvani, L. M. & Davies, H. C. Blocking precursors to stratospheric sudden warming events. *Geophys. Res. Lett.* **36**, L14806 (2009).
35. Huang, J. et al. Preconditioning of arctic stratospheric polar vortex shift events. *J. Clim.* **31**, 5417–5436 (2018).
36. Cellitti, M. P., Walsh, J. E., Rauber, R. M. & Portis, D. H. Extreme cold air outbreaks over the United States, the polar vortex, and the large-scale circulation. *J. Geophys. Res.* **111**, D02114 (2006).
37. Jeong, J.-H. & Ho, C.-H. Changes in occurrence of cold surges over East Asia in association with Arctic Oscillation. *Geophys. Res. Lett.* **32**, L14704 (2005).
38. Thompson, D. W. J. & Wallace, J. M. Regional climate impacts of the northern hemisphere annular mode. *Science* **293**, 85–89 (2001).
39. Wettstein, J. J. & Mearns, L. O. The influence of the north Atlantic–Arctic oscillation on mean, variance, and extremes of temperature in the northeastern United States and Canada. *J. Clim.* **15**, 3586–3600 (2002).
40. Kidston, J. et al. Stratospheric influence on tropospheric jet streams, storm tracks and surface weather. *Nat. Geosci.* **8**, 433–440 (2015).
41. Hartley, D. E., Villarín, J. T., Black, R. X. & Davis, C. A. A new perspective on the dynamical link between the stratosphere and troposphere. *Nature* **391**, 471–474 (1998).
42. Hoskins, B. J., McIntyre, M. E. & Robertson, A. W. On the use and significance of isentropic potential vorticity maps. *Q. J. R. Meteorol. Soc.* **111**, 877–946 (1985).
43. Perlwitz, J. & Harnik, N. Observational evidence of a stratospheric influence on the troposphere by planetary wave reflection. *J. Clim.* **16**, 3011–3026 (2003).
44. Kodera, K., Mukougawa, H. & Fujii, A. Influence of the vertical and zonal propagation of stratospheric planetary waves on tropospheric blockings. *J. Geophys. Res.* **118**, 8333–8345 (2013).
45. Wittman, M. A. H., Charlton, A. J. & Polvani, L. M. The effect of lower stratospheric shear on baroclinic instability. *J. Atmos. Sci.* **64**, 479–496 (2007).
46. Maycock, A. C., Masukwedza, G. I. T., Hitchcock, P. & Simpson, I. R. A regime perspective on the north Atlantic eddy-driven jet response to sudden stratospheric warmings. *J. Clim.* **33**, 3901–3917 (2020).
47. Iwasaki, T. et al. Isentropic analysis of polar cold air mass streams in the northern hemispheric winter. *J. Atmos. Sci.* **71**, 2230–2243 (2014).
48. Yu, Y., Ren, R., Hu, J. & Wu, G. A mass budget analysis on the interannual variability of the polar surface pressure in the winter season. *J. Atmos. Sci.* **71**, 3539–3553 (2014).
49. Yu, Y., Ren, R. & Cai, M. Dynamic linkage between cold air outbreaks and intensity variations of the meridional mass circulation. *J. Atmos. Sci.* **72**, 3214–3232 (2015).
50. Yu, Y., Cai, M., Ren, R. & van den Dool, H. M. Relationship between warm air mass transport into the upper polar atmosphere and cold air outbreaks in winter. *J. Atmos. Sci.* **72**, 349–368 (2015).
51. Cai, M. et al. Feeling the pulse of the stratosphere: an emerging opportunity for predicting continental-scale cold-air outbreaks 1 month in advance. *Bull. Am. Meteor. Soc.* **97**, 1475–1489 (2016).
52. von Eye, A., Wiedermann, W. & Koller, I. Granger Causality: Linear Regression and Logit Models. in *Dependent Data in Social Sciences Research* (eds Stemmler, M., von Eye, A. & Wiedermann, W.) 127–148 (Springer International Publishing, 2015). [https://doi.org/10.1007/978-3-319-20585-4\\_6](https://doi.org/10.1007/978-3-319-20585-4_6).
53. Kobayashi, S. et al. The JRA-55 reanalysis: general specifications and basic characteristics. *J. Meteorol. Soc. Jpn. Ser. II* **93**, 5–48 (2015).
54. Hitchcock, P. On the value of reanalyses prior to 1979 for dynamical studies of stratosphere–troposphere coupling. *Atmos. Chem. Phys.* **19**, 2749–2764 (2019).
55. Ayarzagüena, B. et al. Uncertainty in the response of sudden stratospheric warmings and stratosphere-troposphere coupling to quadrupled CO<sub>2</sub> concentrations in CMIP6 models. *J. Geophys. Res.* **125**, e2019JD032345 (2020).
56. Butler, A. H. et al. Defining sudden stratospheric warmings. *Bull. Am. Meteor. Soc.* **96**, 1913–1928 (2015).
57. Gerber, E. P., Orbe, C. & Polvani, L. M. Stratospheric influence on the tropospheric circulation revealed by idealized ensemble forecasts. *Geophys. Res. Lett.* **36**, L24801 (2009).
58. Charlton-Perez, A. J., Ferranti, L. & Lee, R. W. The influence of the stratospheric state on North Atlantic weather regimes. *Q. J. R. Meteorol. Soc.* **144**, 1140–1151 (2018).
59. Deser, C. On the teleconnectivity of the “Arctic Oscillation”. *Geophys. Res. Lett.* **27**, 779–782 (2000).
60. Hosmer, D. W., Lemeshow, S. & Sturdivant, R. X. *Applied Logistic Regression*. (John Wiley & Sons, 2013).
61. Knight, J. et al. Predictability of European Winters 2017/2018 and 2018/2019: Contrasting influences from the Tropics and stratosphere. *Atmos. Sci. Lett.* **22**, e1009 (2021).
62. Cheung, H. H. N. et al. A strong phase reversal of the Arctic Oscillation in midwinter 2015/2016: role of the stratospheric polar vortex and tropospheric blocking. *J. Geophys. Res.* **121**, 13,443–13,457 (2016).

## Acknowledgements

We thank the editor and two anonymous reviewers for their constructive comments and suggestions which improved the manuscript substantially. This study was supported by the National Science Foundation of China (Grants 42005048 and 41630421). J.H. was funded by the International Postdoctoral Exchange Fellowship Program 2019 by the Office of China Postdoctoral Council (Grants 20190076). C.M.M. and A.C.M. were supported by the European Union’s Horizon 2020 research and innovation program under grant agreement No 820829 (CONSTRAIN project). A.C.M. was supported by the Natural Environment Research Council (NE/M018199/1) and Leverhulme Trust. We thank the scientific teams at Japan Meteorological Agency for providing the reanalysis data and the World Climate Research Program’s Working Group on Coupled Modeling for making CMIP6 model outputs available. Fortran codes for the calculation of cold air mass and its flux in isentropic coordinates provided by Prof. Iwasaki and contributors are highly appreciated.

## Author contributions

J.H. and P.H. designed the research. P.H. collected the CMIP6 data. J.H. performed the data analysis, arranged the results, and wrote the initial draft with a substantial contribution from all other authors. P.H., W.T., A.C.M., and C.M.M. advised on the likelihood of CAOs analysis and interpretation. P.H., A.C.M., C.M.M., and W.T. advised on Granger causality analysis and interpretation. P.H. and W.T. supervised the project. All authors discussed the results and contributed to the paper preparation.

## Competing interests

The authors declare no competing interests.

**Additional information**

**Supplementary information** The online version contains supplementary material available at <https://doi.org/10.1038/s43247-021-00215-6>.

**Correspondence** and requests for materials should be addressed to P.H. or W.T.

**Peer review information** *Communications Earth & Environment* thanks Lukas Papritz and the other, anonymous, reviewer(s) for their contribution to the peer review of this work. Primary Handling Editor: Heike Langenberg. Peer reviewer reports are available.

**Reprints and permission information** is available at <http://www.nature.com/reprints>

**Publisher's note** Springer Nature remains neutral with regard to jurisdictional claims in published maps and institutional affiliations.



**Open Access** This article is licensed under a Creative Commons Attribution 4.0 International License, which permits use, sharing, adaptation, distribution and reproduction in any medium or format, as long as you give appropriate credit to the original author(s) and the source, provide a link to the Creative Commons license, and indicate if changes were made. The images or other third party material in this article are included in the article's Creative Commons license, unless indicated otherwise in a credit line to the material. If material is not included in the article's Creative Commons license and your intended use is not permitted by statutory regulation or exceeds the permitted use, you will need to obtain permission directly from the copyright holder. To view a copy of this license, visit <http://creativecommons.org/licenses/by/4.0/>.

© The Author(s) 2021